Electronic Supplementary Material (ESI) for Physical Chemistry Chemical Physics.
This journal is © the Owner Societies 2015

Supporting Information

Corrole-Ferrocene & Corrole-Anthraquinone Dyads: Synthesis, Spectroscopy and Photochemistry

Jaipal Kandhadi,[a] Venkatesh Yeduru,[ab] Prakriti R. Bangal.[ab*] Lingamallu Giribabu,[ab*]

[*a]Inorganic & Physical Chemistry Division, CSIR-Indian Institute of Chemical Technology, Tarnaka, Hyderabad-500007, Telangana, India.

[*b]Academy of Scientific and Innovative Research (AcSIR), New Delhi, India.

Table of Contents

		Page No.
Fig. S1	ESI-MS spectrum of **Cor-Fc**.	S1
Fig. S2	ESI-MS spectrum of **Cor-AQ**.	S2
Fig. S3	^{1}H NMR spectra of **Cor-Fc** (above) and **Cor-AQ** in $CDCl_3$. The peak labelled with asterisk (*) is due to solvent.	S3
Fig. S4	Absorption spectrum of **Cor-Fc**, **Cor-AQ** along with their constituent monomers in CH_2Cl_2.	S3
Fig. S5	Absorption spectrum of 1:1 mixture of (TTC+Fc) and (TTC+AQ-CHO) along with their constituent monomers in CH_2Cl_2.	S3
Fig. S6	In-situ UV-Visible spectroelectrochemical changes of **Cor-AQ** at its first oxidation potential.	S4
Fig. S7	In-situ UV-Visible spectroelectrochemical changes of **Cor-AQ** at its second oxidation potential.	S4
Fig. S8	In-situ UV-Visible spectroelectrochemical changes of **Cor-Fc** during its first oxidation potential	S5
Fig. S9	In-situ UV-Visible spectroelectrochemical changes of **Cor-Fc** during its second oxidation potential.	S5
Fig. S10	Geometrical optimized structure of **Cor-AQ**, optimized at the B3LYP/6-31G(d) level.	S6
Fig. S11	Geometrical optimized structure of **Cor-Fc**, optimized at the B3LYP/6-31G(d) level.	S6
Fig. S12	Fluorescence spectra λ_{ex}= 425 nm of equi-absorbing solutions (O. D. λ_{ex} =	S7

0.05).

Fig. S13 Transient absorption spectra of **TTC** λ_{Pump} =575 nm in ACN., Inset shows time profile at 480 nm. S8

Fig. S14 Kinetic at 435, 465 and 525 nm upon 410 nm excitation of **TTC**. S8

Fig. S15 Kinetic at 435, 465 and 525 nm upon 575 nm excitation of **TTC**. S9

Fig. S16 Transient absorption Spectra of **Cor-AQ** dyad in ACN upon 575 nm excitation S9

Fig. S17 Probe wavelength dependent kinetic profile of **Cor-AQ** (A) and **Cor-Fc** (B) dyads upon 410 nm excitation in ACN. S10

Fig. S18. Comparison of **Cor-AQ** fluorescence upconversion signal decay vs excited state absorption decay for two different excitations

Fig.S19 Comparison of **Cor-Fc** fluorescence upconversion signal decay vs excited state absorption decay for two different excitations

Fig.S20. Comparative analysis of transient absorption spectra of TTC 1ps after pump to $EADS_1$ of Cor-AQ and Cor-FC. ΔOD has been arbitrarily scaled for better comparison of spectral shape.

Fig.S21. Evolution-associated difference spectra (EADS) resulting from the global fitting applying a sequential model to the femtosecond transient absorption data of **Cor-AQ** (A) and **Cor-Fc** (B)

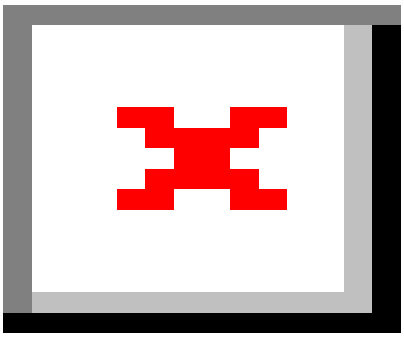

Figure S1. ESI-MS spectrum of **[Cor-Fc]**.

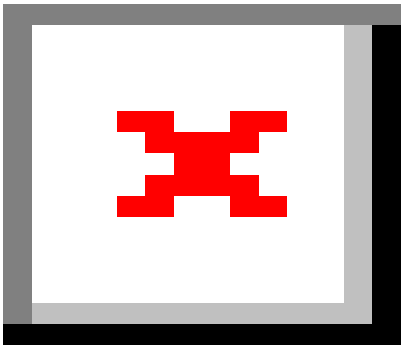

Figure S2. ESI-MS spectrum of **[Cor-AQ]**.

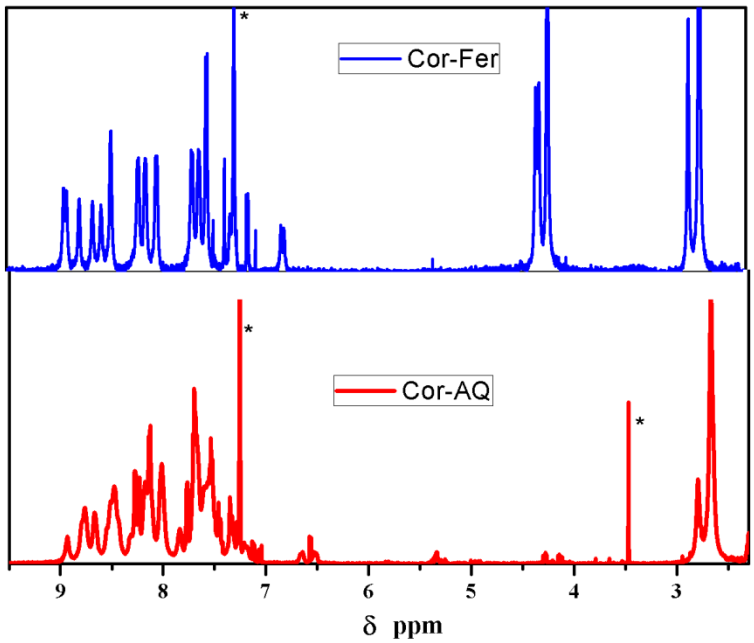

Figure S3. ^{1}H NMR spectra of **Cor-Fc** (above) and Cor-AQ in $CDCl_3$. The peak labelled with asterisk (*) is due to solvent.

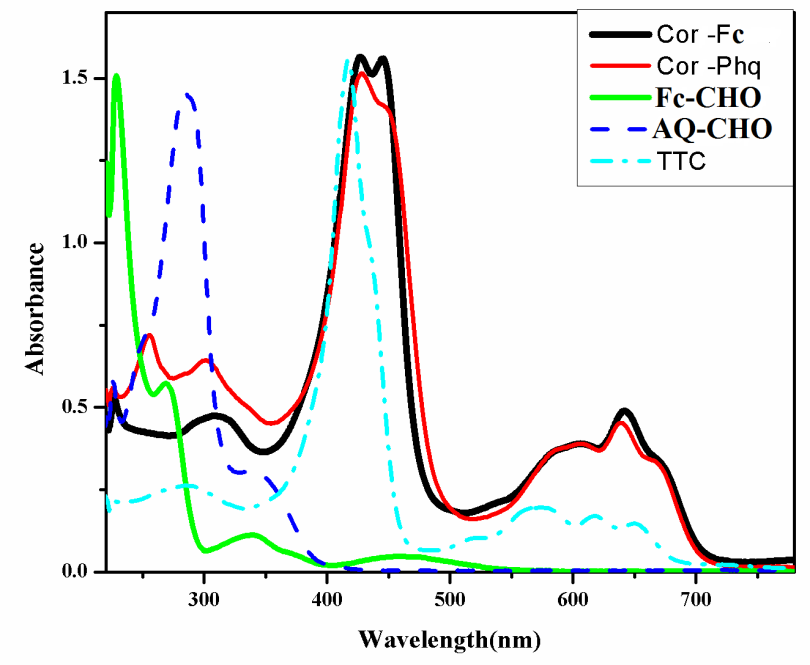

Figure S4. Absorption spectrum of **Cor-Fc**, **Cor-AQ** along with their constituent monomers in CH_2Cl_2.

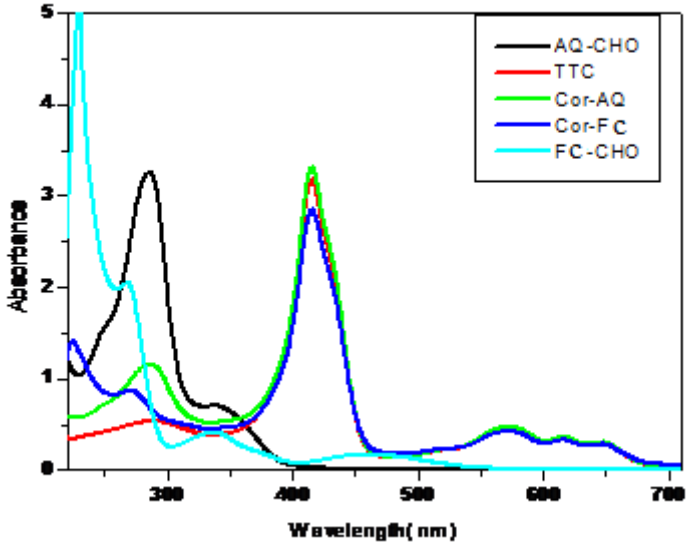

Figure S5. Absorption spectrum of 1:1 mixture of (TTC+Fc) and (TTC+AQ-CHO) along with their constituent monomers in CH_2Cl_2.

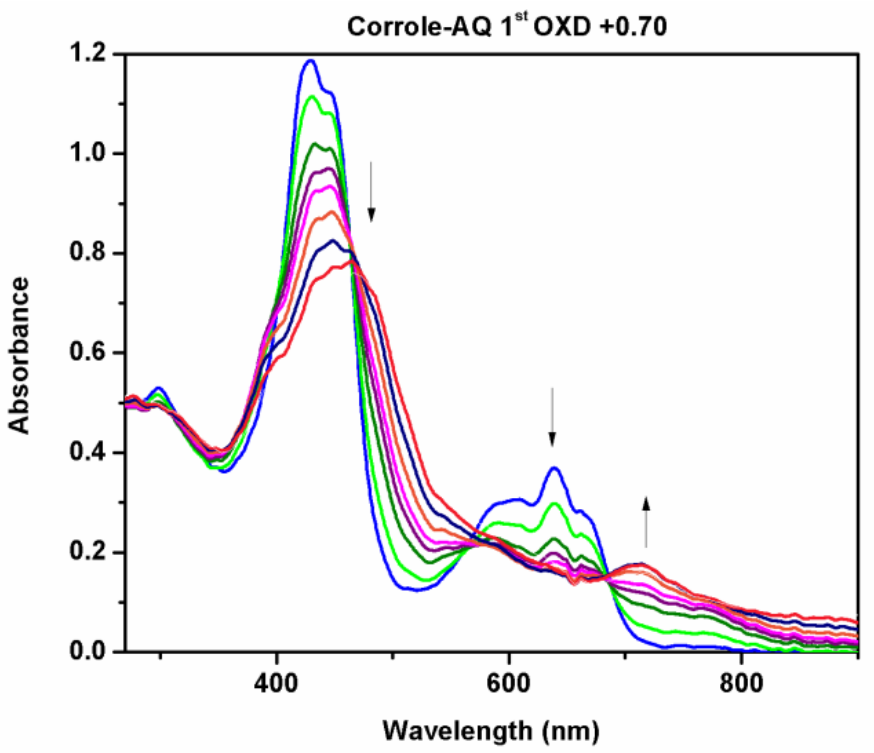

Figure S6. In-situ UV-Visible spectroelectrochemical changes of (Cor-AQ) at its first oxidation potential.

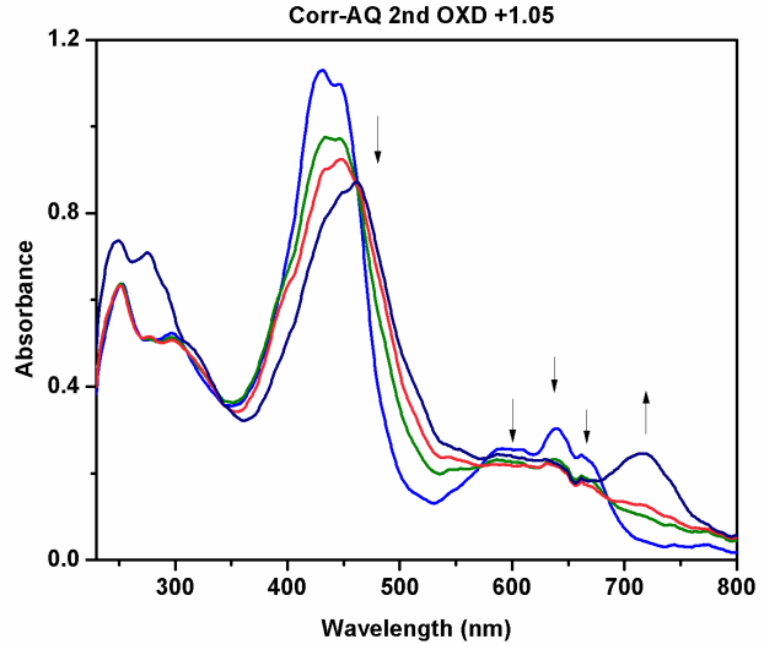

Figure S7. In-situ UV-Visible spectroelectrochemical changes of (Cor-AQ) at its second oxidation potential.

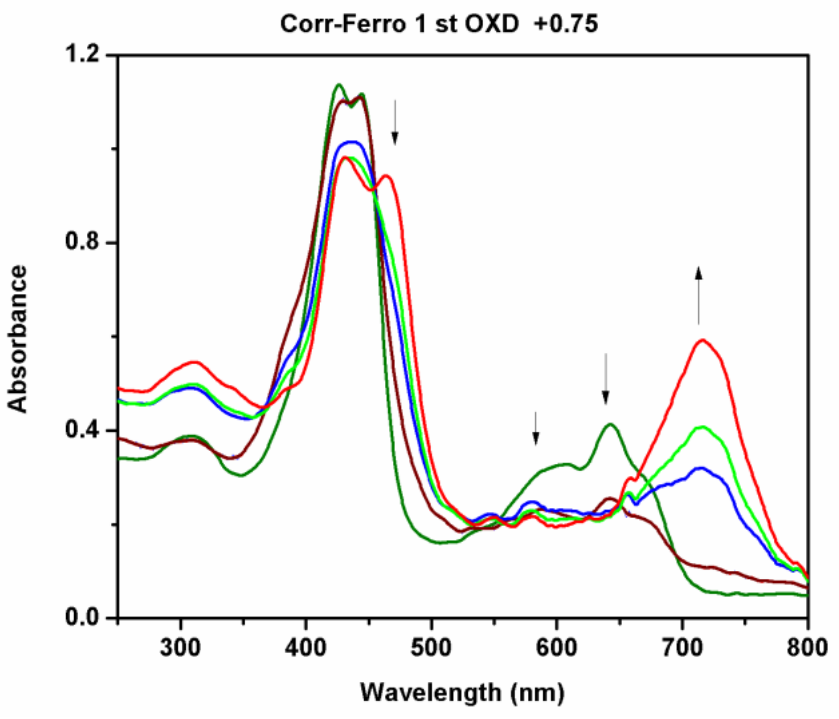

Figure S8. In-situ UV-Visible spectroelectrochemical changes of **(Cor-Fer)** during its first oxidation potential.

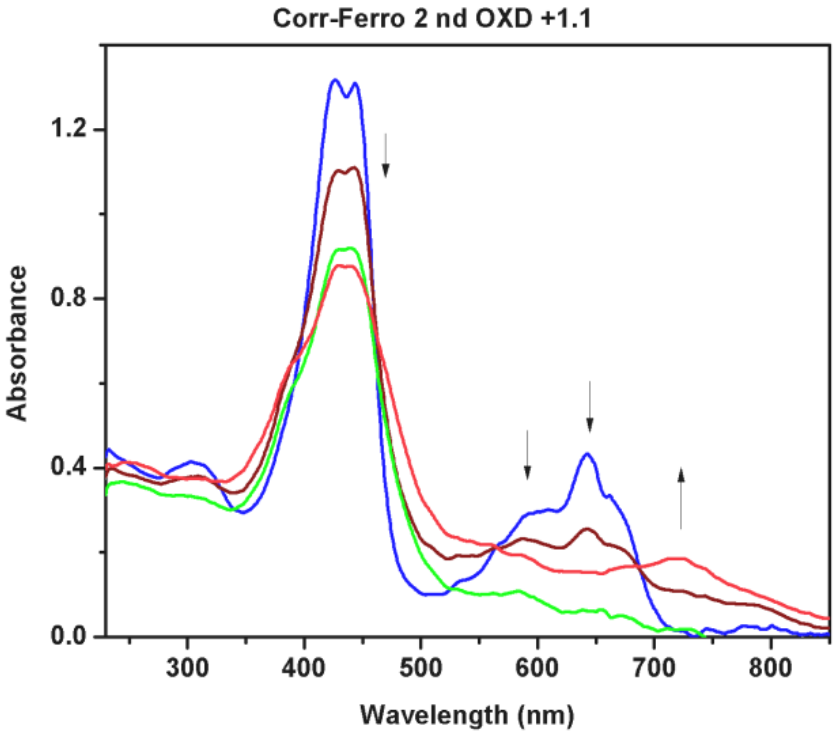

Figure S9. In-situ UV-Visible spectroelectrochemical changes of **(Cor-Fc)**during its second oxidation potential.

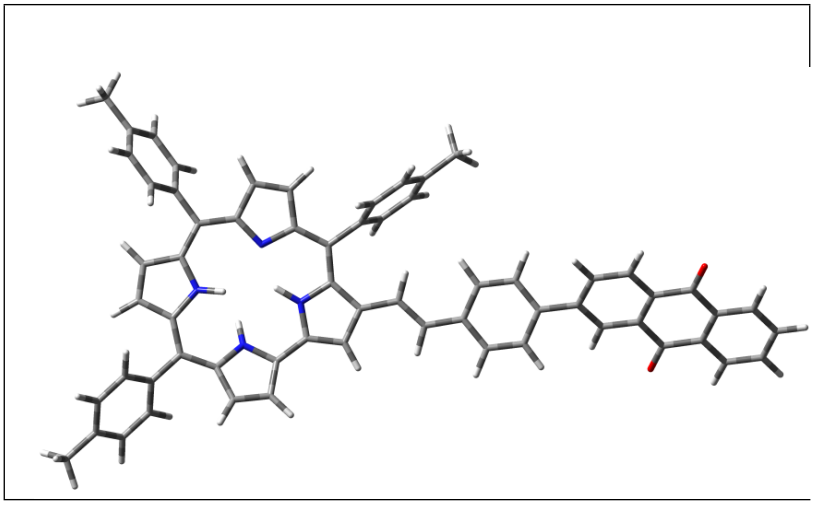

Figure S10. Geometrical optimized structure of (**Cor-AQ**), optimized at the B3LYP/6-31G(d)level.

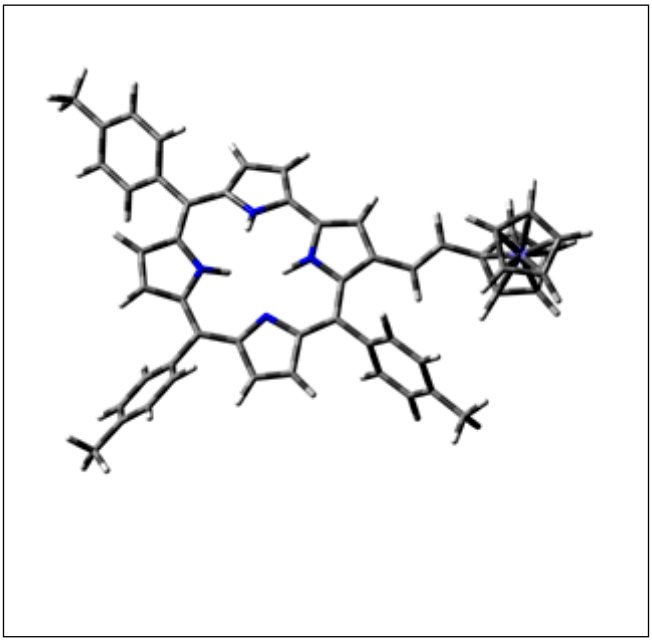

Figure S11. Geometrical optimized structure of (**Cor-Fc**), optimized at the B3LYP/6-31G(d) level.

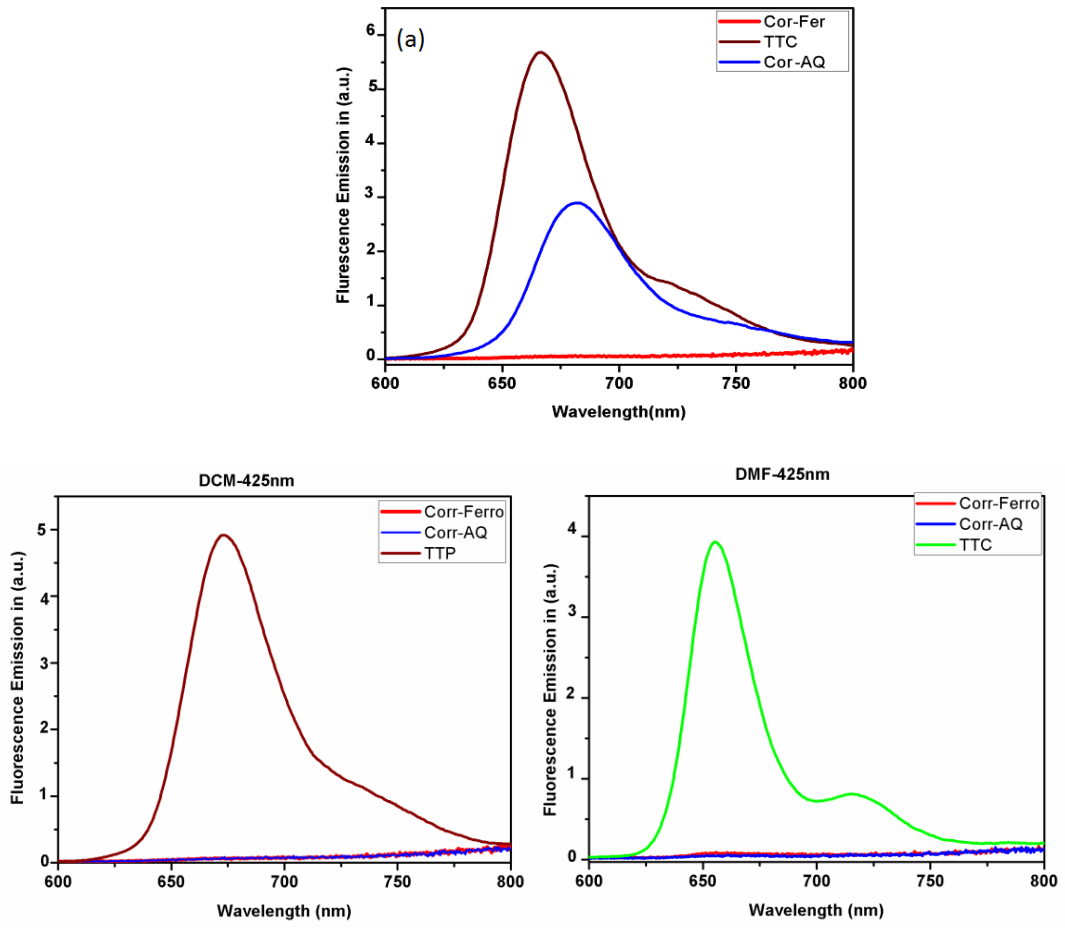

Figure S12. Fluorescence spectra λ_{ex}= 425 nm of equi-absorbing solutions (O. D. λ_{ex} = 0.05).

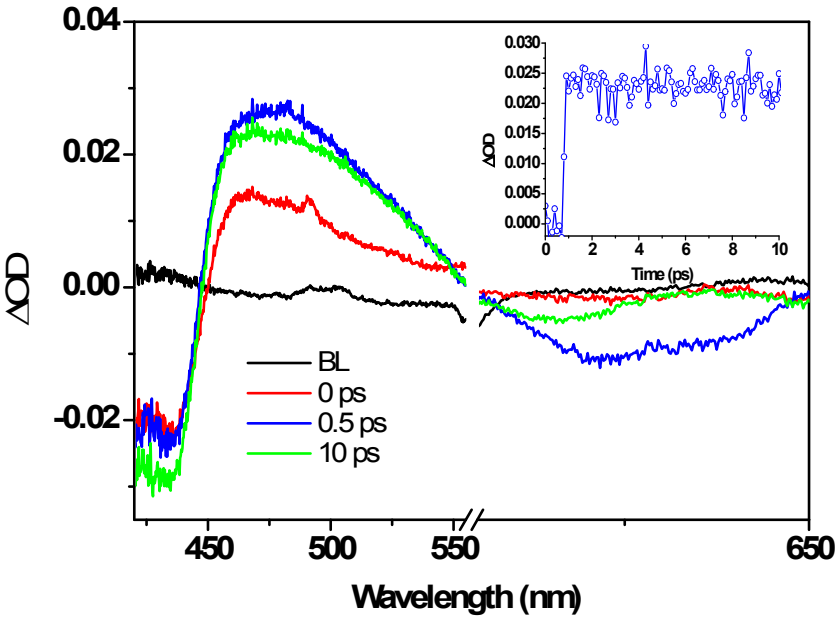

Figure S13. Transient absorption spectra of **TTC** λ_{Pump} =575 nm in ACN., Inset shows time profile at 480 nm.

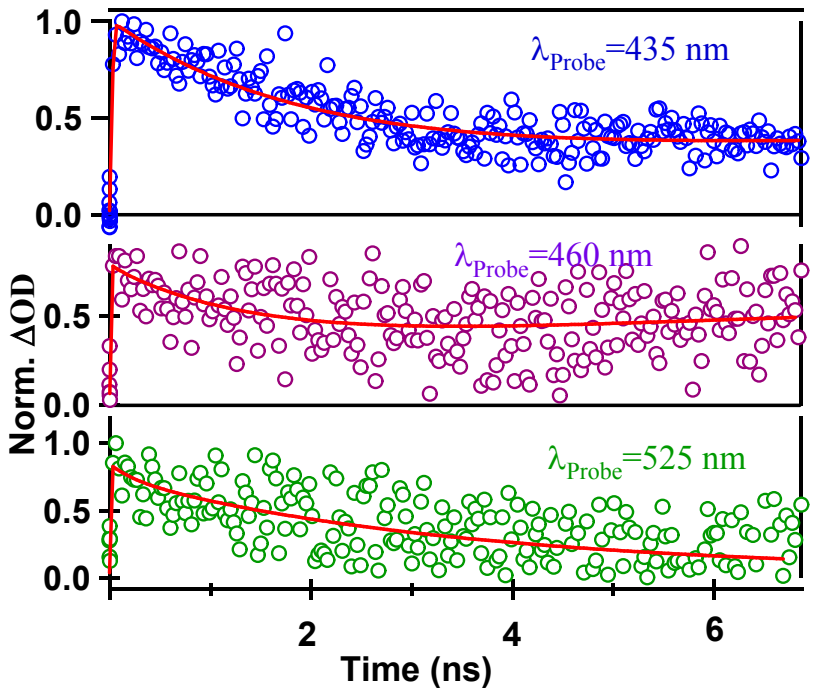

Figure S14. Kinetic at 435, 465 and 525 nm upon 410 nm excitation of TTC in 6.5 ns time window..

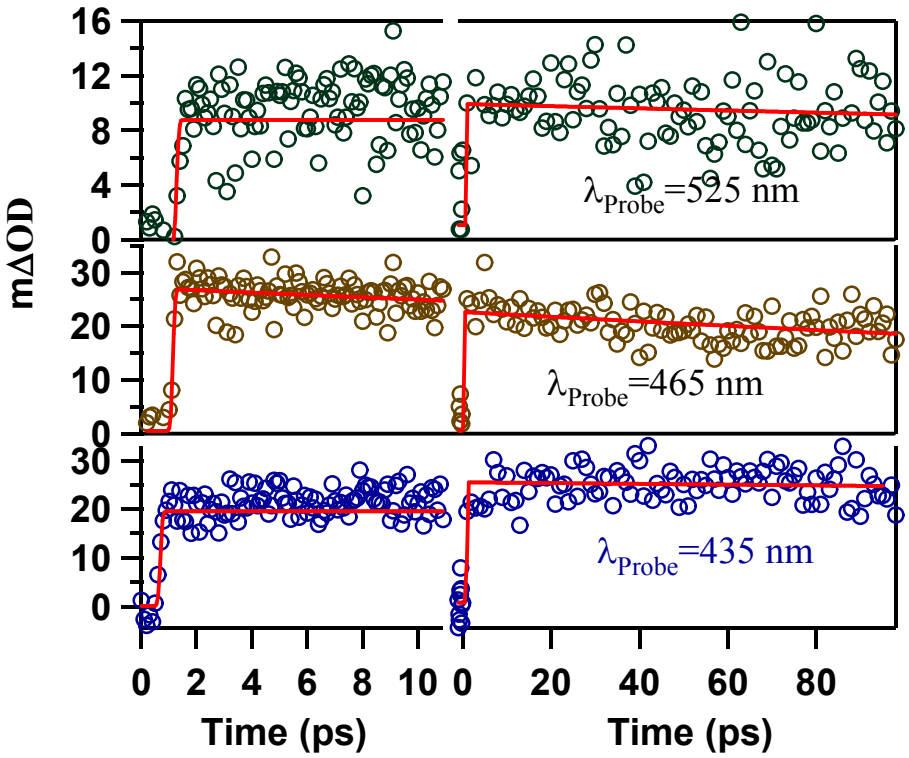

Figure S15. Kinetic at 435, 465 and 525 nm upon 575 nm excitation of **TTC**.

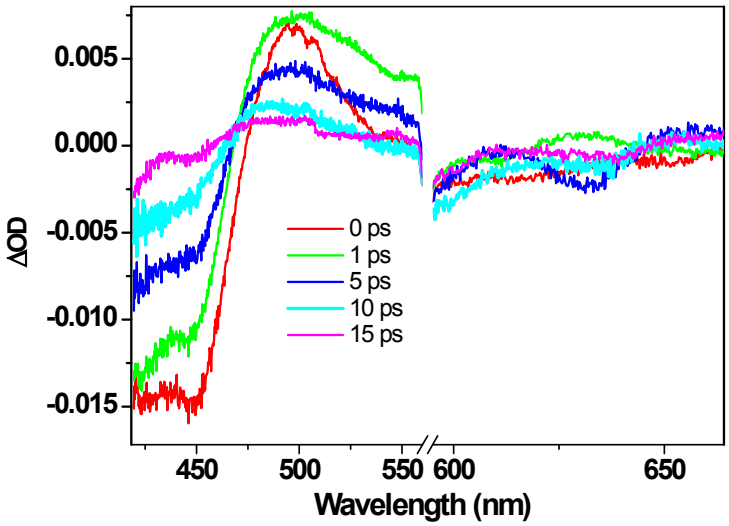

Figure S16. Transient absorption Spectra of **Cor-AQ** dyad in ACN upon 575 nm excitation.

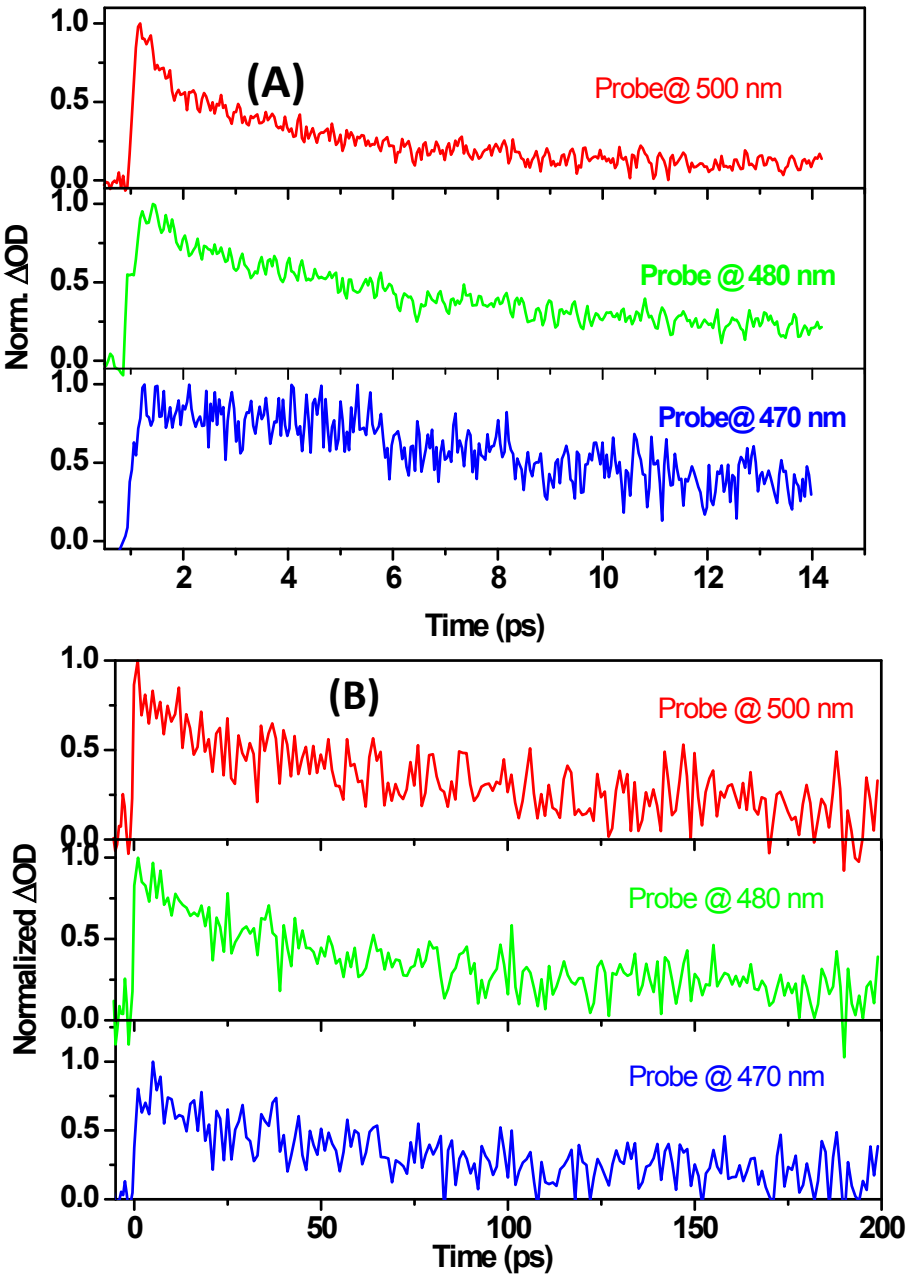

Figure S17. Probe wavelength dependent kinetic profile of (**Cor-AQ**) (A) and (**Cor-Fc**) (B) dyads upon 410 nm excitation in ACN.

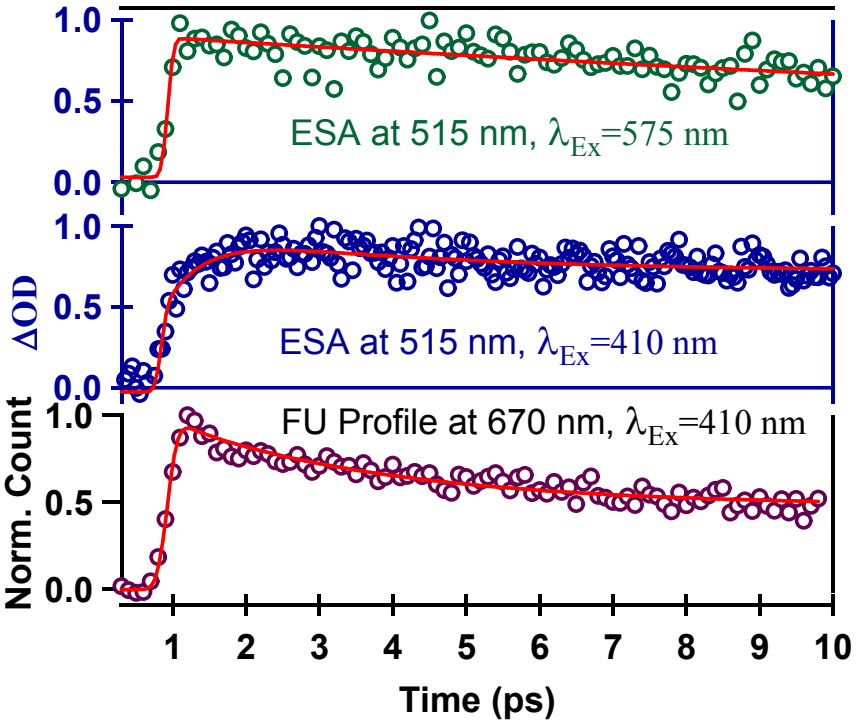

Figure S18. Comparison of **Cor-AQ** fluorescence up-conversion signal decay vs excited state absorption decay for two different excitations .

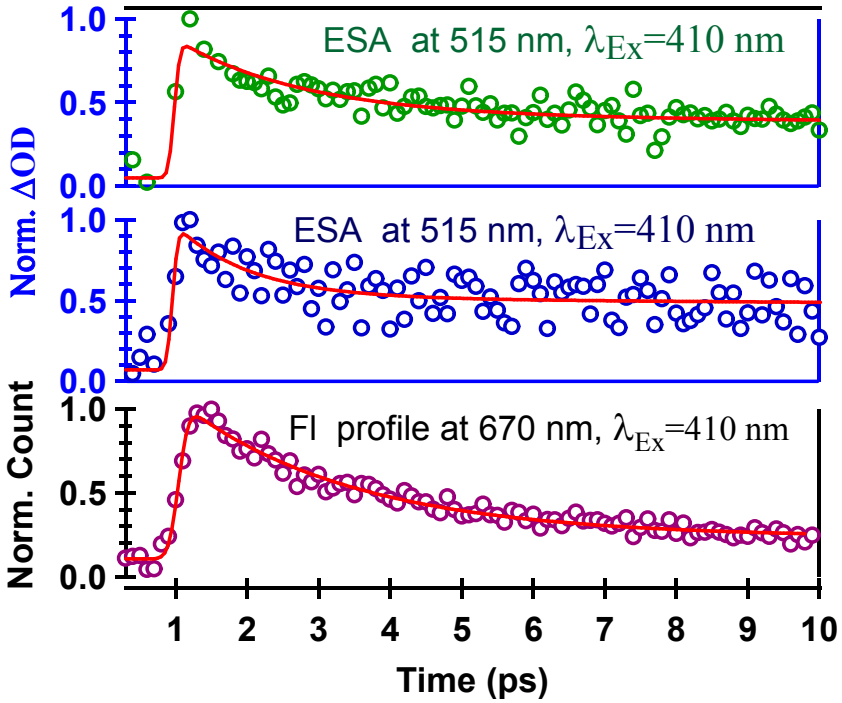

Figure S19. Comparison of **Cor-Fc** fluorescence upconversion signal decay vs excited state absorption decay for two different excitations.

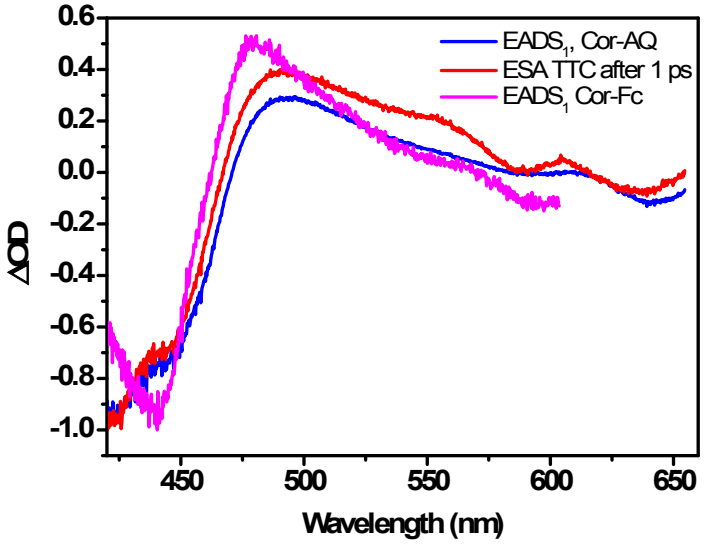

Figure S20. Comparative analysis of transient absorption spectra of TTC 1ps after pump to $EADS_1$ of Cor-AQ and Cor-FC. ΔOD has been arbitrarily scaled for better comparison of spectral shape.

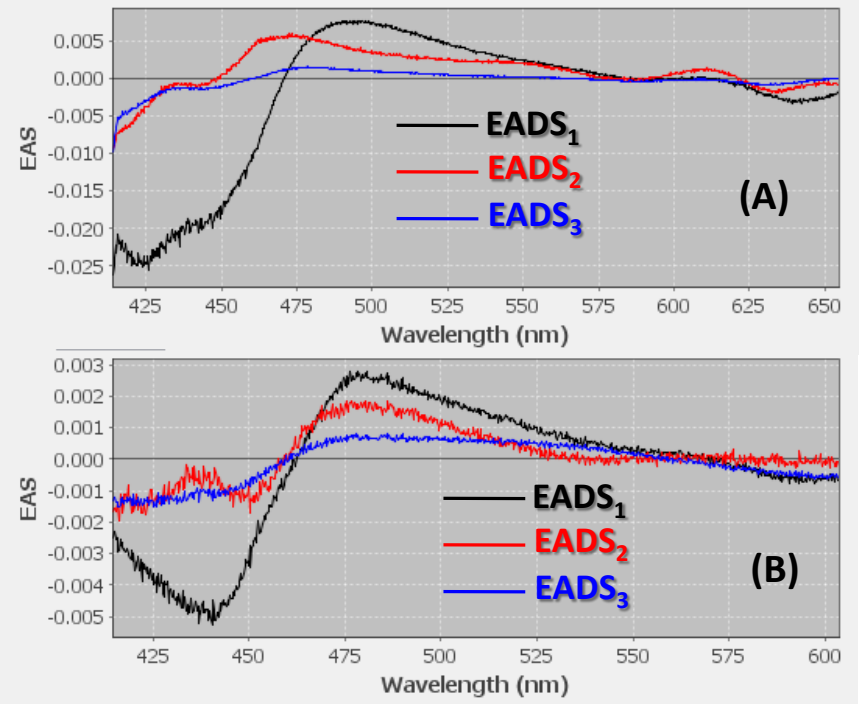

Figure S 21. Evolution-associated difference spectra (EADS) resulting from the global fitting applying a sequential model to the femtosecond transient absorption data of **Cor-AQ** (A) and **Cor-Fc** (B)